

Entropy generation analysis of two-dimensional high-temperature confined jet

S.X. Chu, L.H. Liu *

School of Energy Science and Engineering, Harbin Institute of Technology, 92 West Dazhi Street, Harbin 150001, People's Republic of China

Received 14 September 2007; received in revised form 30 June 2008; accepted 1 July 2008

Available online 31 July 2008

Abstract

In high-temperature systems, thermal radiation becomes the dominant mode of heat transfer. The analysis of entropy generation mechanism is very important to optimize the second-law performance of these energy conversion devices. In this paper, the entropy generation in a two-dimensional high-temperature confined jet flow is analyzed. The computation of combined radiation and convection heat transfer is carried out with the help of a CFD code, and the entropy generation due to heat transfer and fluid friction is calculated as post-processed quantities with the computed data of velocity, temperature and radiative intensity. Numerical results show the entropy generation due to radiative transfer cannot be omitted in high-temperature systems such as boilers and furnaces, in which thermal radiation is one of the main modes of heat transfer. In the case that the temperatures of the inlet gas and the top and bottom are not changed, the total entropy generation number decreases with the increase of jet Reynolds number and Boltzmann number, respectively. For enhancing heat transfer and advancing energy conversion efficiency, large jet Reynolds number and Boltzmann number should be selected.

© 2008 Elsevier Masson SAS. All rights reserved.

Keywords: Entropy generation; Radiative heat transfer; High-temperature system; Jet flow

1. Introduction

The second law of thermodynamics has extensive application in problems involving heat transfer and fluid flow. Entropy generation is associated with thermodynamic irreversibility, which is present in all heat transfer and fluid flow processes. Bejan [1–3] developed the concept and the methodology of entropy generation minimization. The minimization of entropy generation in heat transfer and fluid flow equipments provides considerable improvement in efficient operation.

Recently, considerable research work has been carried out to understand the mechanism of entropy generation in heat transfer and fluid flow processes. Balaji et al. [4] examined the role of buoyancy in the total entropy generation rate in turbulent mixed convection flows. Ko and Ting [5] analyzed the entropy generation induced by forced convection in a curved rectangular duct with external heating. Ko and Cheng [6] in-

vestigated the entropy generation in the developing laminar forced convection within a wavy channel, and analyzed the effects of Reynolds number on entropy generation. Based on the Reynolds-average transport equation, Kock and Herwig [7] studied the local entropy production in turbulent shear flows. Hooman et al. [8] analyzed heat transfer and entropy generation optimization of forced convection in porous-saturated ducts of rectangular cross-section. Due to the low temperature level within the heat transfer devices considered in these studies, in which heat convection is the dominant mode of heat transfer, the effect of thermal radiation was often omitted.

In many high-temperature systems such as solar collectors, boilers and furnaces, thermal radiation becomes the dominant mode of heat transfer. The analysis of entropy generation mechanism is very important to optimize the second-law performance of these energy conversion devices. The second law analysis in combustion processes was carried out by many researchers, for example, Raghavan et al. [9], Nishida et al. [10], Arpacı and Selamet [11], Datta [12], Datta and Som [13], Yapıcı et al. [14]. Theoretically, the effect of thermal radiation needs to be considered in the analysis of entropy generation

* Corresponding author. Tel.: +86 451 86402237.
E-mail address: lhliu@hit.edu.cn (L.H. Liu).

Nomenclature

| | | | | | |
|-----------------------------|--|--|-----------------------------|---|----------------------------------|
| A | surface area of boundary | m^2 | $\dot{S}_{\text{gen},f}'''$ | volumetric entropy generation rate due to viscous dissipation | $\text{W m}^{-3} \text{K}^{-1}$ |
| Bo | Boltzmann number | | $\dot{S}_{\text{gen},r}'''$ | volumetric entropy generation rate due to radiative transfer in gas | $\text{W m}^{-3} \text{K}^{-1}$ |
| c_0 | speed of light in vacuum | m/s | $\dot{S}_{\text{gen},r}''A$ | entropy generation rate per unit area due to radiative transfer at wall | $\text{W m}^{-2} \text{K}^{-1}$ |
| c_P | specific heat at constant pressure | $\text{J kg}^{-1} \text{K}^{-1}$ | S_G^c | total entropy generation due to heat conduction and convection | W K^{-1} |
| d | height of the spout | m | S_G^f | total entropy generation due to viscous dissipation | W K^{-1} |
| h | Planck's constant | J s | S_G^r | total entropy generation due to radiative heat transfer in gas | W K^{-1} |
| H | height of the duct | m | S_G^A | total entropy generation due to wall radiation | W K^{-1} |
| I_λ | spectral radiative intensity | $\text{W m}^{-3} \text{sr}^{-1}$ | S_G | total entropy generation | W K^{-1} |
| $I_{b,\lambda}$ | spectral radiative intensity of blackbody | $\text{W m}^{-3} \text{sr}^{-1}$ | T | matter temperature | K |
| k | turbulent kinetic energy | $\text{m}^2 \text{s}^{-2}$ | T_0 | environment temperature | K |
| k_b | Boltzmann's constant | J K^{-1} | T_{ref} | reference temperature | K |
| k_m | thermal conductivity of gas | $\text{W m}^{-1} \text{K}^{-1}$ | T_λ | spectral radiation temperature | K |
| k_{eff} | effective thermal conductivity | $\text{W m}^{-1} \text{K}^{-1}$ | u | velocity component in x -direction | m s^{-1} |
| L | length of the duct | m | u_{in} | axial inlet velocity of jet | m s^{-1} |
| L_λ | spectral radiative entropy intensity | $\text{W m}^{-3} \text{sr}^{-1} \text{K}^{-1}$ | v | velocity component in y -direction | m s^{-1} |
| $L_{b,\lambda}$ | spectral radiative entropy intensity of blackbody | $\text{W m}^{-3} \text{sr}^{-1} \text{K}^{-1}$ | V | volume | m^3 |
| \mathbf{n}_w | unit outward normal vector of boundary wall | | x, y | Cartesian coordinates | m |
| N_S | total entropy generation number | | y_P | distance between the solid wall and the closest node | |
| N_{S_c} | entropy generation number due to heat conduction and convection | | ε | emissivity | |
| N_{S_f} | entropy generation number due to viscous dissipation | | $\kappa_{a,\lambda}$ | spectral absorption coefficient | m^{-1} |
| N_{S_r} | entropy generation number due to radiative heat transfer in gas | | $\kappa_{s,\lambda}$ | spectral scattering coefficient | m^{-1} |
| N_{S_A} | entropy generation number due to wall radiation | | λ | wavelength | μm |
| \mathbf{q} | heat flux vector | W m^{-2} | μ_m | dynamic viscosity of gas | $\text{kg m}^{-1} \text{s}^{-1}$ |
| Q | total heat transfer rate of the system | W | μ_{eff} | effective dynamic viscosity | $\text{kg m}^{-1} \text{s}^{-1}$ |
| \mathbf{r} | position vector | m | μ_t | turbulent viscosity | $\text{kg m}^{-1} \text{s}^{-1}$ |
| Re_d | jet Reynolds number | | ρ | density | kg m^{-3} |
| \mathbf{s} | direction vector | | Φ | single scattering phase function | |
| $\dot{S}_{\text{gen},c}'''$ | volumetric entropy generation rate due to heat conduction and convection | $\text{W m}^{-3} \text{K}^{-1}$ | Ω | solid angle | sr |

in high-temperature systems. Unfortunately, even for the high-temperature reacting flows in combustion devices, up to now the thermal radiation is still not taken into account in the analysis of entropy generation.

Traditionally, the local entropy generation rate for radiative heat transfer is often written as [15–19]

$$\dot{S}_{\text{gen},r}'''(\mathbf{r}) = -\mathbf{q}^r(\mathbf{r}) \cdot \frac{\nabla T(\mathbf{r})}{T^2(\mathbf{r})} \quad (1)$$

where T is temperature, \mathbf{q}^r is the radiative heat flux vector. Liu and Chu [20] checked the formula of entropy generation used in the community of heat transfer, and found that traditional conduction-type formula of entropy generation rate cannot be used to calculate the local entropy generation rate of radiative heat transfer. Based on Planck's definition of radiative entropy [21], Caldas and Semiao [22] deduced the transfer equation of radiative entropy and presented a numerical simula-

tion method of radiative entropy generation in the participating medium. Liu and Chu [23] extended this method to analyze the radiative entropy generation in the enclosures filled with semi-transparent media.

In this paper, based on the radiative entropy generation formula given in Refs. [22,23], we study the entropy generation in a two-dimensional high-temperature confined jet flow. The computation of combined radiation and convection heat transfer is carried out with the help of CFD code Fluent 6.1.22, and the local entropy generation due to heat transfer and fluid friction is calculated as post-processed quantities with the computed data of velocity, temperature and radiative intensity. The distributions of entropy generation due to heat conduction and convection, thermal radiation transfer in gas and viscous fluid friction are analyzed, and the effect of jet Reynolds number, Boltzmann

number and wall emissivity on entropy generation in the high-temperature confined jet flow are studied, respectively.

2. Mathematical formulae and method of simulation

As shown in Fig. 1, the problem under consideration is a two-dimensional symmetric confined plane jet flow. The heights of the duct and the spout are $H = 0.4$ m and $d = 0.06$ m, respectively, and the length of the duct simulated in the following is $L = 1.0$ m. A carbon dioxides jet with temperature $T_{in} = 1000$ K is sprayed into the duct. The top and the bottom boundaries of the duct are opaque walls with temperature $T_w = 500$ K, respectively, but the left boundary of the duct is an adiabatic wall. The environment temperature is $T_0 = 500$ K.

The thermal conductivity, molecular viscosity, density and specific heat of carbon dioxide in FLUENT 6.1.22 are given by $k_m = 0.0145$ W/mK, $\mu_m = 1.37 \times 10^{-5}$ kg/ms, $\rho = 1.7878$ kg/m³ and $c_p = 840.37$ J/kg K, respectively. The kinematic coefficient of viscosity is $\nu = \mu/\rho$. When inlet velocity of gas is $u_{in} = 1$ m/s, the Reynolds number at the nozzle of spout is $Re_d = u_{in}d/\nu = 7830$. In the following analysis, $u_{in} \geq 1$ m/s, thus the jet flow is turbulent. The turbulence intensity at the inlet can be specified by

$$I = 0.16(Re_d)^{-1/8} \quad (2)$$

2.1. Calculation tools

The FLUENT 6.1.22 program was chosen as the CFD computer code for this work. The FLUENT computer code uses a finite volume procedure to solve the Navier–Stokes equations of fluid flow in primitive variables such as velocity and pressure. This computer code also can model the radiative heat transfer of semitransparent medium by solving radiative transfer equation [24–27].

The standard $k-\varepsilon$ model has been usually used to simulate the turbulent flow with no swirl for its efficiency [27–29]. Because the flow considered here has no swirl and the standard $k-\varepsilon$ model required short computing time compared with the others, we use the standard $k-\varepsilon$ model to simulate the turbulent jet flow in this paper. For the region of flow parameter considered in this paper, the distance between the solid wall and the closest node, y_p , meets the following condition

$$11.5 \leq \frac{y_p C_\mu^{1/4} k^{1/2}}{\nu} \leq 200 \quad (3)$$

Hence, we adopt the standard wall function for handling the wall-bounded turbulent flow problems considered here.

The P-1 radiation model was adopted in Refs. [24–26] to model radiative heat transfer for its low computational requirements and simplicity. However, the accuracy of P-1 radiation model is only appropriate to optical thickness medium [30]. The discrete ordinates method (DOM) is widely used to model radiative heat transfer for its better accuracy [31–34]. So we select the DOM for the computation model of radiative heat transfer in FLUENT software.

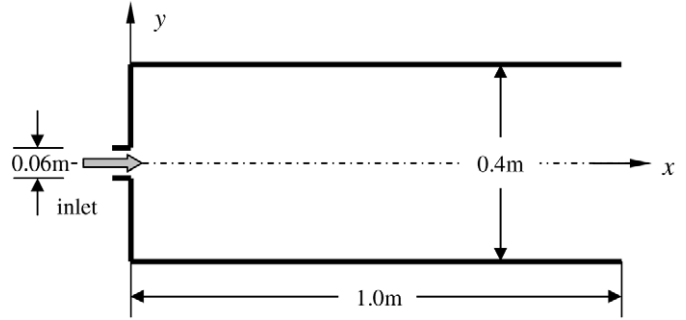


Fig. 1. Geometry of turbulent confined jet.

After the velocity and temperature distributions are solved using the FLUENT computer code. The local entropy generation due to heat conduction, heat convection and fluid friction is calculated as post-processed quantities with the computed data of velocity and temperature. The radiative intensity and then the local entropy generation due to radiative transfer are solved using the DOM (S_8) with the temperature data.

The assumptions made in the following analysis are as follows:

- (1) The confined jet flow is steady, two-dimensional symmetric, turbulent and incompressible;
- (2) The carbon dioxides is assumed to behave as an ideal gas with absorption coefficient $\kappa_a = 0.43$;
- (3) No-slip condition is assumed at the solid walls;
- (4) The gradients of velocity, temperature, turbulent kinetic energy and turbulent energy dissipation rate are zero at the outlet of duct;
- (5) The inlet and the outlet boundaries are assumed as black-body with the same temperature as local fluid medium for the solution of radiative transfer equation [35,36].

2.2. Local entropy generation rate

In the high-temperature non-reacting jet, irreversibility arises due to the heat transfer and the viscous effects of the fluid. The local volumetric entropy generation rate can be expressed as the sum of contributions due to thermal effects and viscous effects. The viscous effects depend on the local velocity gradient of fluid, and the local entropy generation of heat conduction and convection is dependent on the local temperature gradient of the fluid. However, because thermal radiation is a long-range phenomenon, the local radiative heat transfer and the entropy generation rate are dependent on the temperature distribution of the entire enclosure under consideration and are not determined by the local temperature gradient.

Similar to the method adopted in Ref. [14], in this paper the local entropy generation of viscous dissipation and that of heat conduction and convection are determined by effective dynamic viscosity and effective thermal conductivity, respectively, in which the effective dynamic viscosity and the effective thermal conductivity are defined respectively as

$$\mu_{\text{eff}} = \mu_m + \mu_t \quad (4)$$

$$k_{\text{eff}} = k_m + \frac{c_p \mu_t}{Pr_t} \quad (5)$$

where Pr_t is turbulent Prandtl number, and μ_t is turbulent dynamic viscosity given by

$$\mu_t = \rho C_\mu \frac{k^2}{\varepsilon} \quad (6)$$

Here, C_μ is 0.09, and k is turbulent kinetic energy.

In the two-dimensional high-temperature and non-reacting flow system, the volumetric entropy generation rate per unit volume can be written as:

$$\dot{S}_{\text{gen}}''' = \dot{S}_{\text{gen},c}''' + \dot{S}_{\text{gen},f}''' + \dot{S}_{\text{gen},r}''' \quad (7)$$

where $\dot{S}_{\text{gen},c}'''$, $\dot{S}_{\text{gen},f}'''$ and $\dot{S}_{\text{gen},r}'''$ denote the volumetric entropy generation rates due to the heat conduction and convection, the viscous fluid friction and the thermal radiative transfer in carbon dioxide gas flow, respectively, and they are given as

$$\dot{S}_{\text{gen},c}''' = \frac{k_{\text{eff}}}{T^2} (\nabla T)^2 \quad (8)$$

$$\dot{S}_{\text{gen},f}''' = \frac{\mu_{\text{eff}}}{T} \left\{ 2 \left[\left(\frac{\partial u_x}{\partial x} \right)^2 + \left(\frac{\partial u_y}{\partial y} \right)^2 \right] + \left(\frac{\partial u_x}{\partial y} + \frac{\partial u_y}{\partial x} \right)^2 \right\} \quad (9)$$

$$\begin{aligned} \dot{S}_{\text{gen},r}''' = & \int_0^\infty \int_{4\pi} \left[-(\kappa_{a,\lambda} + \kappa_{s,\lambda}) \frac{I_\lambda(\mathbf{r}, \mathbf{s})}{T_\lambda(\mathbf{r}, \mathbf{s})} + \kappa_{a,\lambda} \frac{I_{b,\lambda}(\mathbf{r})}{T_\lambda(\mathbf{r}, \mathbf{s})} \right. \\ & \left. + \frac{\kappa_{s,\lambda}}{4\pi} \int_{4\pi} \frac{I_\lambda(\mathbf{r}, \mathbf{s}')}{T_\lambda(\mathbf{r}, \mathbf{s})} \Phi(\mathbf{s}', \mathbf{s}) d\Omega' \right] d\Omega d\lambda \\ & + \int_0^\infty \int_{4\pi} \frac{\kappa_{a,\lambda}}{T(\mathbf{r})} [I_\lambda(\mathbf{r}, \mathbf{s}) - I_{b,\lambda}(\mathbf{r})] d\Omega d\lambda \end{aligned} \quad (10)$$

Here the spectral radiation temperature corresponding to spectral radiative intensity $I_\lambda(\mathbf{r}, \mathbf{s})$ is defined as

$$T_\lambda(\mathbf{r}, \mathbf{s}) = \frac{hc_0}{\lambda k_b} \frac{1}{\ln[2hc_0^2 \lambda^{-5} / I_\lambda(\mathbf{r}, \mathbf{s}) + 1]} \quad (11)$$

where, \mathbf{r} is spatial position vector, and \mathbf{s} is direction vector, Ω is solid angle, λ is wavelength, c_0 is the speed of light in vacuum, h is Planck's constant, k_b is Boltzmann's constant, $\kappa_{a,\lambda}$ and $\kappa_{s,\lambda}$ are spectral absorption and scattering coefficients, respectively.

In addition to the entropy generation due to absorption and scattering in semitransparent medium, the irreversibility of wall absorption and emission processes also lead to entropy generation. The entropy generation rate per unit area due to wall absorption and emission processes can be written as:

$$\dot{S}_{\text{gen},r}''A = \int_0^\infty \int_{4\pi} \left[\frac{I_\lambda(\mathbf{r}_w, \mathbf{s})}{T(\mathbf{r}_w)} - L_\lambda(\mathbf{r}_w, \mathbf{s}) \right] (\mathbf{n}_w \cdot \mathbf{s}) d\Omega d\lambda \quad (12)$$

where L_λ is the spectral radiation entropy intensity corresponding to spectral radiative intensity I_λ and defined as

$$\begin{aligned} L_\lambda(\mathbf{r}_w, \mathbf{s}) = & 2k_b c_0 \lambda^{-4} \left\{ \left(\frac{I_\lambda(\mathbf{r}_w, \mathbf{s})}{2hc_0^2 \lambda^{-5}} + 1 \right) \ln \left(\frac{I_\lambda(\mathbf{r}_w, \mathbf{s})}{2hc_0^2 \lambda^{-5}} + 1 \right) \right. \\ & \left. - \left(\frac{I_\lambda(\mathbf{r}_w, \mathbf{s})}{2hc_0^2 \lambda^{-5}} \right) \ln \left(\frac{I_\lambda(\mathbf{r}_w, \mathbf{s})}{2hc_0^2 \lambda^{-5}} \right) \right\} \end{aligned} \quad (13)$$

2.3. Total entropy generation and entropy generation number

The total entropy generation due to the heat conduction and convection, the viscous dissipation and the radiative heat transfer in gas can be derived by integrating Eqs. (8), (9) and (10) over volume as follows:

$$S_G^c = \int_V \dot{S}_{\text{gen},c}''' dV \quad (14)$$

$$S_G^f = \int_V \dot{S}_{\text{gen},f}''' dV \quad (15)$$

$$S_G^r = \int_V \dot{S}_{\text{gen},r}''' dV \quad (16)$$

By integrating Eq. (12) over boundary area, the total entropy generation due to wall radiative heat transfer can be written as

$$S_G^A = \int_A \dot{S}_{\text{gen},r}''A dA \quad (17)$$

and the total entropy generation of the jet system consider here is

$$S_G = S_G^c + S_G^f + S_G^r + S_G^A \quad (18)$$

In the second law analysis of heat transfer and flow processes the entropy generation number is often used to evaluate the irreversibility of the process. In the following analysis, the entropy generation number due to heat conduction and convection, viscous dissipation, radiative heat transfer in gas and that due to wall radiation are defined respectively as

$$Ns_c = \frac{S_G^c T_0}{Q} \quad (19)$$

$$Ns_f = \frac{S_G^f T_0}{Q} \quad (20)$$

$$Ns_r = \frac{S_G^r T_0}{Q} \quad (21)$$

$$Ns_A = \frac{S_G^A T_0}{Q} \quad (22)$$

where, Q is the total heat transfer rate of the system. The total entropy generation number of the system can be written as

$$Ns = Ns_c + Ns_f + Ns_r + Ns_A = \frac{S_G T_0}{Q} \quad (23)$$

3. Results and discussion

Grid-refinement studies were also performed for the physical model to ensure that the essential physics are independent of grid size. The axial velocity profiles and the corresponding axial temperature profiles for five different grid numbers, namely, $N_x \times N_y = 101 \times 41$, 141×57 , 201×81 , 261×105 and 301×121 , are shown in Fig. 2. The numerical results show that, when the nodes number is equal to or larger than 261×105 , the numerical results are very close to one another. Therefore, we adopt 261×105 nodes for all the following calculations.

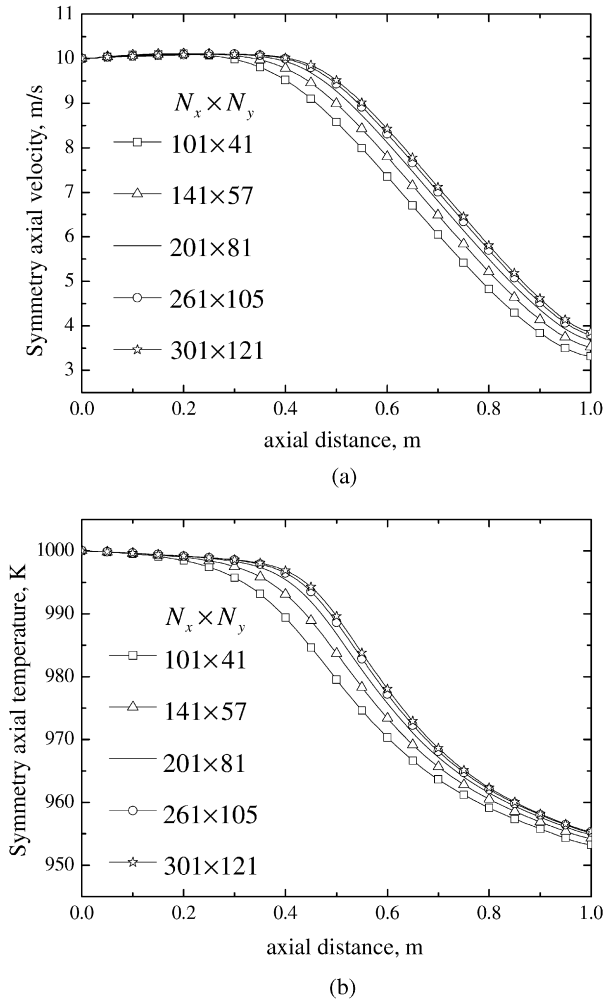


Fig. 2. Distribution of gas velocity and temperature on symmetry axis for different nodes: (a) axial velocity; (b) temperature.

3.1. Distribution of entropy generation

In this section we analyze the distribution of entropy generation due to heat conduction and convection, viscous dissipation and radiative transfer in the system for the case of $Re_d = 78298$ and $\varepsilon = 1.0$. The volumetric entropy generation rate due to heat conduction and convection and that due to viscous dissipation are related to the distributions of temperature and velocity, respectively. Fig. 3 shows the typical flow structure of the turbulent confined jet. The computed contour lines of temperature and velocity are depicted in Figs. 4 and 5, respectively. Figs. 6 and 7 depict the distribution of volumetric entropy generation rate due to heat conduction and convection and that due to viscous dissipation, respectively. As shown in Figs. 6 and 7, generally the volumetric entropy generation rate due to heat conduction and convection is larger than that due to viscous dissipation in the case considered in this paper.

As shown in Fig. 4, the temperature gradient can be neglected at the jet core zone where the gas temperature is kept the same as the inlet gas temperature. At the beginning section of the mixing layer, the strong turbulent perturbation owing to gas entrainment leads to large temperature gradients. The

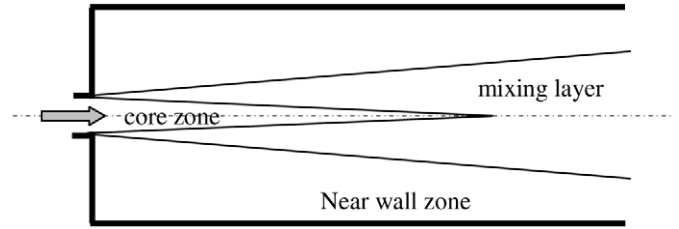


Fig. 3. Flow structure of the turbulent confined jet.

mixing layer expands along the direction of jet flow, and the temperature gradient gradually decreases. Therefore, as shown in Fig. 6, the volumetric entropy generation rate due to heat conduction and convection gradually decreases from the center to the edge of mixing layer. The volumetric entropy generation rate due to heat conduction and convection in the center of mixing layer is larger than $100 \text{ W}/(\text{m}^3 \text{ K})$, and the maximum value of volumetric entropy generation rate due to heat conduction and convection is $789.32 \text{ W}/(\text{m}^3 \text{ K})$. From the edge of mixing layer to solid wall, due to the effect of boundary layer, the temperature gradient and hence the volumetric entropy generation rate due to heat conduction and convection increase gradually. The volumetric entropy generation rate due to heat conduction and convection is larger than $1000 \text{ W}/(\text{m}^3 \text{ K})$ in the narrow zone close to the isothermal wall, and the maximum value of volumetric entropy generation rate is $8236.16 \text{ W}/(\text{m}^3 \text{ K})$. The thickness of this narrow zone is about $3.846 \times 10^{-3} \text{ m}$ and the entropy generation due to heat conduction and convection in this zone is about 80.88% of the total entropy generation due to heat conduction and convection. The volumetric entropy generation due to heat conduction and convection is small and less than $20 \text{ W}/(\text{m}^3 \text{ K})$ in the most zones of the computational domain.

As shown in Figs. 5 and 7, because of low velocity gradient the volumetric entropy generation rate due to viscous dissipation is small at the jet core zone. Similar to heat conduction and convection processes, owing to the gas entrainment phenomena the velocity gradient is large at the center of mixing layer. This indicates that the volumetric entropy generation rate due to viscous dissipation is larger in the center of mixing layer than that at the other zones. From the center to the edge of mixing layer, the velocity gradient decreases gradually. Therefore, the volumetric entropy generation rate due to viscous dissipation gradually decreases from the center to the edge of mixing layer.

Fig. 8 shows the distribution of volumetric radiation entropy generation rate. The largest value of volumetric radiation entropy generation rate is located at the jet core zone, in which the temperature difference between gas and solid wall is the larger than that at the other zones. By comparison with Figs. 6, 7 and 8, it can be seen that, generally, the volumetric entropy generation due to heat conduction and convection is larger than that due to the radiative transfer in gas and the viscous dissipation near boundary layer. However, the volumetric radiation entropy generation is not small in whole zone.

The entropy generation due to heat conduction and convection dominates in the case of $Re_d = 78298$ and $\varepsilon = 1$, which is 67.97% of total entropy generation of the system considered

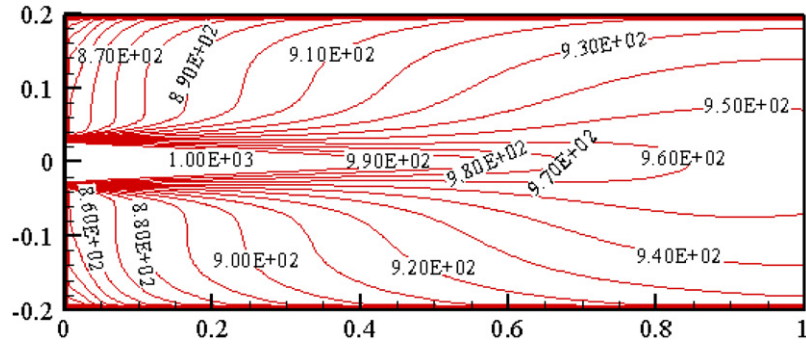


Fig. 4. Computed contour lines of gas temperature (K).

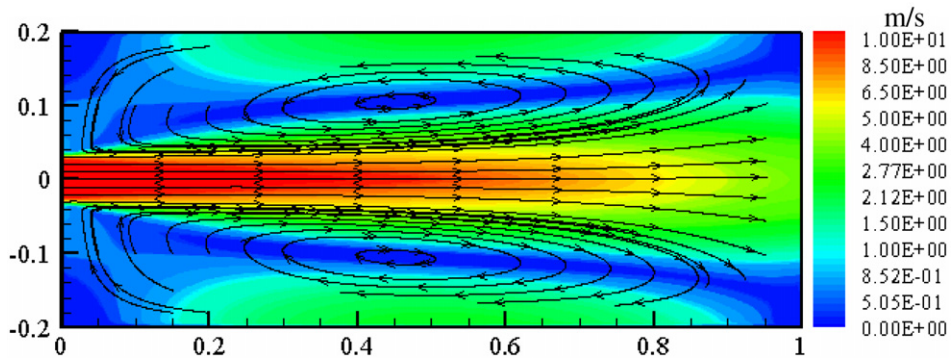


Fig. 5. Distribution of gas velocity and the stream lines.

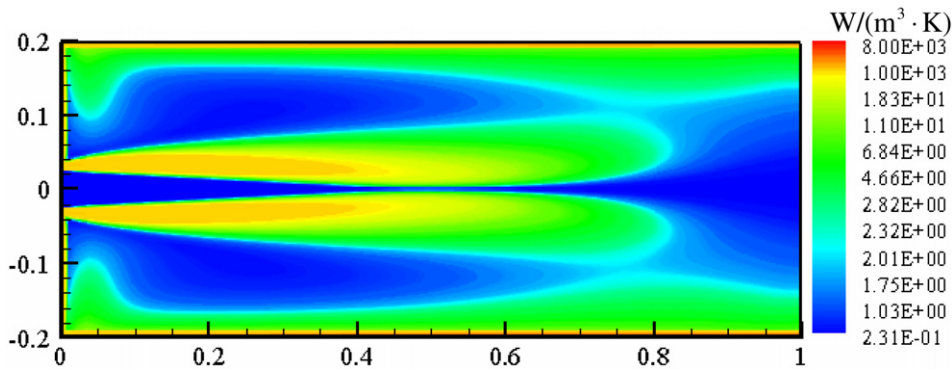


Fig. 6. Distribution of volumetric entropy generation rate due to heat conduction and convection.

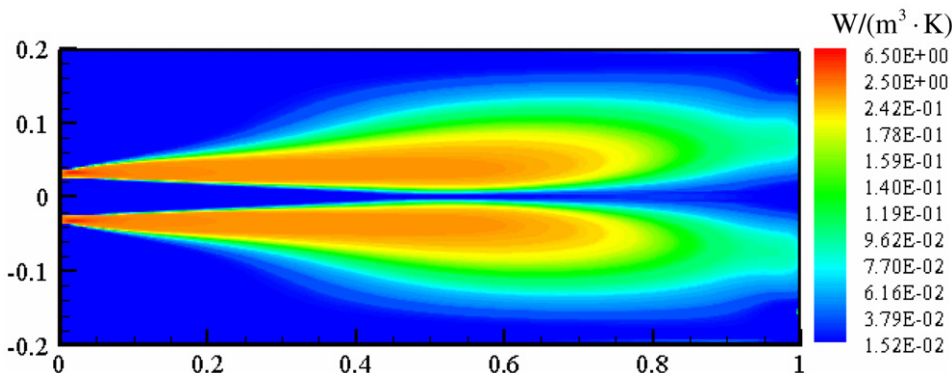


Fig. 7. Distribution of volumetric entropy generation rate due to viscous dissipation.

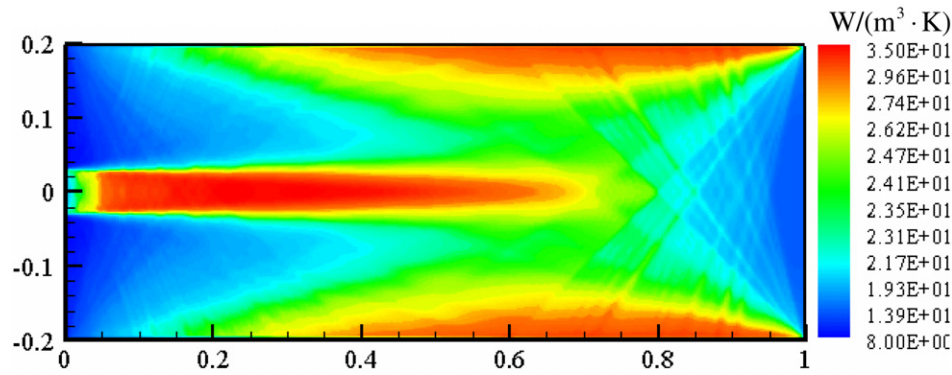


Fig. 8. Distribution of volumetric entropy generation rate due to radiative transfer in gas.

Table 1

Apportioning of total entropy generation and their percents for different jet Reynolds number in the case of wall emissivity $\varepsilon = 1.0$

| Re_d | S_G^c/S_G (%) | S_G^f/S_G (%) | S_G^r/S_G (%) | S_G^A/S_G (%) | S_G (W/K) | N_s |
|--------|-----------------|-----------------------|-----------------|-----------------|-------------|-------|
| 7830 | 27.95 | 2.03×10^{-4} | 26.18 | 45.86 | 21.54 | 0.33 |
| 15660 | 37.31 | 1.05×10^{-3} | 21.70 | 40.99 | 31.96 | 0.25 |
| 39149 | 54.20 | 9.12×10^{-3} | 15.24 | 30.56 | 54.91 | 0.17 |
| 78298 | 67.97 | 0.04 | 10.43 | 21.56 | 87.66 | 0.14 |
| 117447 | 75.17 | 0.11 | 7.97 | 16.75 | 118.81 | 0.13 |
| 156596 | 79.61 | 0.21 | 6.46 | 13.72 | 149.51 | 0.12 |

Table 2

Apportioning of total entropy generation and their percents for different wall emissivity in the case of jet Reynolds number $Re_d = 78298$

| ε | S_G^c/S_G (%) | S_G^f/S_G (%) | S_G^r/S_G (%) | S_G^A/S_G (%) | S_G (W/K) | N_s |
|---------------|-----------------|-----------------|-----------------|-----------------|-------------|-------|
| 0.4 | 67.10 | 0.04 | 13.88 | 18.97 | 89.64 | 0.141 |
| 0.6 | 67.31 | 0.04 | 12.42 | 20.23 | 88.91 | 0.140 |
| 0.8 | 67.61 | 0.04 | 11.31 | 21.03 | 88.25 | 0.139 |
| 1.0 | 67.97 | 0.04 | 10.43 | 21.56 | 87.66 | 0.138 |

here. Radiation entropy generation includes the entropy generation due to gas radiation process and that due to wall radiation process. The percent of wall radiation entropy generation in the total entropy generation is 21.56%. Unlike the entropy generation due to heat conduction and convection, the volumetric entropy generation rate due to radiative transfer in gas is quite even and larger than $8 \text{ W}/(\text{m}^3 \text{ K})$ in the most zones of the computational domain. The radiation entropy generation in gas is 10.43% of the total entropy generation. Hence the percent of entropy generation due to radiative transfer in the total entropy generation is 31.99%. Therefore, the entropy generation due to radiative transfer cannot be omitted in high-temperature systems such as boilers and furnaces, in which thermal radiation is one of the main modes of heat transfer.

3.2. Effect of jet Reynolds number on entropy generation

To better understand the effect of jet Reynolds number on entropy generation and total entropy generation number, Table 1 shows the apportioning of total entropy generation in the case of $\varepsilon = 1$. Within the Reynolds number region considered in this paper, the entropy generation due to viscous dissipation is small, and its percent in total entropy generation of the system is less than 0.5%. The total entropy generation increases

quickly with the jet Reynolds number. However, with the increase of the jet Reynolds number, the heat transfer process is enhanced, and hence the total entropy generation number decreases in the case that the temperatures of the inlet gas and the top and bottom are not changed. The percent of the entropy generation due to heat conduction and convection increases with the jet Reynolds number from 27.95 to 79.61%, but the percent of radiation entropy generation decreases with the increase of jet Reynolds number from 21.56 to 10.43%. Even in the case of $Re_d = 156596$, the entropy generation due to radiative heat transfer in the high temperature system still cannot be neglected.

3.3. Effect of wall emissivity on entropy generation

Table 2 shows the constitutions of total entropy generation and their percents for different wall emissivity in the case of the jet Reynolds number $Re_d = 78298$. Both of the total entropy generation and the total entropy generation number decrease with the increase of wall emissivity. However, in the case that the temperatures of the inlet gas and the top and bottom are not changed, the variations of the total entropy generation and the total entropy generation number are small. From Table 2, it can be clearly seen that the percent of entropy generation due to heat

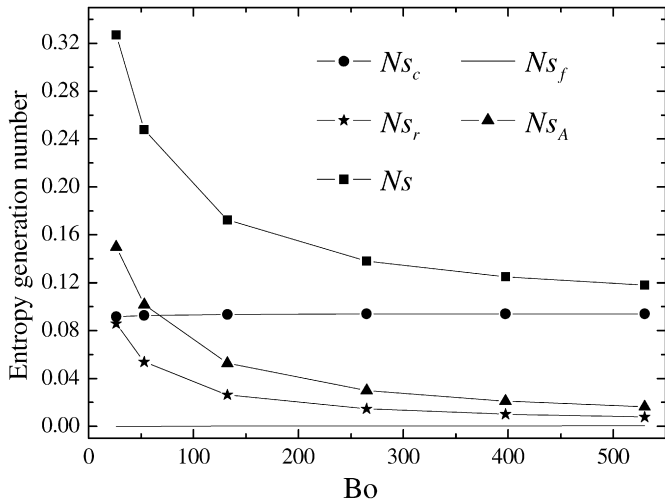


Fig. 9. Effect of Boltzmann number on entropy generation number in the case of $\varepsilon = 1$.

conduction and convection and that due to viscous dissipation varies slowly with the increase of wall emissivity.

3.4. Effect of Boltzmann number on entropy generation

Boltzmann number approximately reflects the ratio of heat convection and radiation, which is defined as

$$Bo = \frac{\rho c_p u_{in}}{\sigma T_{ref}^3} \quad (24)$$

Here T_{ref} is the reference temperature, which is selected the same value as the inlet temperature of gas, i.e., $T_{ref} = 1000$ K. Fig. 9 shows the distribution of entropy generation number with Boltzmann number in the case of $\varepsilon = 1$. With the increase of Boltzmann number, the variation of entropy generation number due to heat conduction and convection and that due to viscous dissipation are negligible, but the entropy generation number due to radiative heat transfer in gas and that due to wall radiation decrease first quickly (in the region of $Bo < 200$) and then decrease slowly (in the region of $Bo > 200$).

From the analysis above, attention should be paid near wall zone and the center of mixing layer where the local heat conduction and convection entropy generation rate per unit volume is large, and radiation entropy generation should be taken into account for enhancing heat transfer and advancing energy conversion efficiency in high-temperature systems. The total entropy generation number would be minimized by adopting large jet Reynolds number and Boltzmann number.

4. Conclusions

Entropy generation is associated with thermodynamic irreversibility, which is present in all heat transfer and fluid flow processes. Based on the radiative entropy generation formula given in Refs. [22,23], we studied the entropy generation in a two-dimensional high-temperature confined jet flow. The computation of combined radiation and convection heat transfer was carried out with the help of CFD code Fluent 6.1.22, and the

local entropy generation rates due to heat transfer and fluid friction were calculated as post-processed quantities with the computed data of velocity, temperature and radiative intensity. The main conclusions from present analysis can be summarized as follows:

- (1) The entropy generation due to radiative transfer cannot be omitted in high-temperature systems such as boilers and furnaces, in which thermal radiation is one of the main modes of heat transfer.
- (2) In the case that the temperatures of the inlet gas and the top and bottom are not changed, the total entropy generation number decreases with the increase of jet Reynolds number and Boltzmann number, respectively.
- (3) The effect of wall emissivity on total entropy generation and total entropy generation number is small.
- (4) For enhancing heat transfer and advancing energy conversion efficiency, large jet Reynolds number and Boltzmann number should be selected.

Acknowledgements

The support of this work by the National Natural Science Foundation of China (50425619) and the Science Fund of Heilongjiang Province for Distinguished Young Scholars (No. JC04-03) is gratefully acknowledged.

References

- [1] A. Bejan, *Entropy Generation Through Heat and Fluid Flow*, Wiley, New York, 1982.
- [2] A. Bejan, *Entropy Generation Minimization*, CRC Press, New York, 1996.
- [3] A. Bejan, *Advanced Engineering Thermodynamics*, second ed., Wiley, New York, 1997.
- [4] C. Balaji, M. Holling, H. Herwig, Entropy generation minimization in turbulent mixed convection flows, *International Communications in Heat and Mass Transfer* 34 (2007) 544–552.
- [5] T.H. Ko, K. Ting, Entropy generation and optimal analysis for laminar forced convection in curved rectangular ducts: A numerical study, *International Journal of Thermal Sciences* 45 (2006) 138–150.
- [6] T.H. Ko, C.S. Cheng, Numerical investigation on developing laminar forced convection and entropy generation in a wavy channel, *International Communications in Heat and Mass Transfer* 34 (2007) 924–933.
- [7] F. Kock, H. Herwig, Local entropy production in turbulent shear flows: A high-Reynolds number model with wall functions, *International Journal of Heat and Mass Transfer* 47 (2004) 2205–2215.
- [8] K. Hooman, H. Gurgenci, A.A. Merrikh, Heat transfer and entropy generation optimization of forced convection in porous-saturated ducts of rectangular cross-section, *International Journal of Heat and Mass Transfer* 50 (2007) 2051–2059.
- [9] V. Raghavan, G. Gogos, V. Babub, T. Sundararajan, Entropy generation during the quasi-steady burning of spherical fuel particles, *International Journal of Thermal Sciences* 46 (2007) 589–604.
- [10] K. Nishida, T. Takagi, S. Kinoshita, Analysis of entropy generation and exergy loss during combustion, *Proceeding of the Combustion Institute* 39 (2002) 869–874.
- [11] V.S. Arpaci, A. Selamet, Entropy production in flames, *Combustion and Flame* 73 (1988) 251–259.
- [12] A. Datta, Entropy generation in a confined lamina diffusion flame, *Combustion Science and Technology* 159 (2000) 39–56.
- [13] A. Datta, S.K. Som, Thermodynamic irreversibilities and second law analysis in a spray combustion process, *Combustion Science and Technology* 142 (1999) 29–54.

- [14] H. Yapıcı, N. Kayatas, B. Albayrak, G. Basturk, Numerical calculation of local entropy generation in a methane—air burner, *Energy Conversion and Management* 46 (2005) 1885–1919.
- [15] V.S. Arpaci, Radiative entropy production, *AIAA Journal* 24 (1986) 1859–1860.
- [16] V.S. Arpaci, Radiative entropy production—lost heat into entropy, *International Journal of Heat and Mass Transfer* 30 (1987) 2115–2123.
- [17] V.S. Arpaci, A. Esmaeeli, Radiative deformation, *Journal of Applied Physics* 87 (2000) 3093–3100.
- [18] V.S. Arpaci, Thermal deformation: from thermodynamics to heat transfer, *Journal of Heat Transfer* 123 (2001) 821–826.
- [19] V.S. Arpaci, Radiative entropy production—heat lost to entropy, *Adv. Heat Transfer* 21 (1991) 239–276.
- [20] L.H. Liu, S.X. Chu, On the entropy generation formula of radiation heat transfer, *Journal of Heat Transfer* 128 (2006) 504–506.
- [21] M. Planck, *The Theory of Heat Radiation*, Dover Publications, New York, 1959.
- [22] F. Caldas, V. Semiao, Entropy generation through radiative transfer in participating media: Analysis and numerical computation, *Journal of Quantitative Spectroscopy and Radiative Transfer* 96 (2005) 423–437.
- [23] L.H. Liu, S.X. Chu, Verification of numerical simulation method for entropy generation of radiation heat transfer in semitransparent medium, *Journal of Quantitative Spectroscopy and Radiative Transfer* 103 (2007) 43–56.
- [24] R. Vuthaluru, H.B. Vuthaluru, Modelling of a wall fired furnace for different operating conditions using FLUENT, *Fuel Processing Technology* 87 (2006) 633–639.
- [25] S.P. Khare, T.F. Wall, et al., Factors influencing the ignition of flames from air-fired swirl pf burners retrofitted to oxy-fuel, *Fuel* 87 (2008) 1042–1049.
- [26] A. Habibi, B. Merci, G.J. Heynderickx, Impact of radiation models in CFD simulations of steam cracking furnaces, *Computers and Chemical Engineering* 31 (2007) 1389–1406.
- [27] M. Ilbas, The effect of thermal radiation and radiation models on hydrogen-hydrocarbon combustion modeling, *International Journal of Hydrogen Energy* 30 (2005) 1113–1126.
- [28] M. Ilbas, I. Yilmaz, T.N. Veziroglu, Y. Kaplan, Hydrogen as burner fuel: Modeling of hydrogen-hydrocarbon composite fuel combustion and NOx formation in a small burner, *International Journal of Energy Research* 29 (2005) 973–990.
- [29] M. Ilbas, I. Yilmaz, Y. Kaplan, Investigations of hydrogen and hydrogen-hydrocarbon composite fuel combustion and NOx emission characteristics in a model combustor, *International Journal of Hydrogen Energy* 30 (2005) 1139–1147.
- [30] M.F. Modest, *Radiative Heat Transfer*, second ed., Academic Press, San Diego, CA, 2003.
- [31] M. Sakami, A. Charette, V.L. Dez, Application of the discrete ordinates method to combined conductive and radiative heat transfer in a two-dimensional complex geometry, *Journal of Quantitative Spectroscopy and Radiative Transfer* 56 (1996) 517–533.
- [32] N. Kayakol, Performance of discrete ordinates method in a gas turbine combustor simulation, *Experimental Thermal and Fluid Science* 21 (2001) 134–141.
- [33] K.A.R. Ismail, C.T.S. Salinas, Gray radiative conductive 2D modeling using discrete ordinates method with multidimensional spatial scheme and non-uniform grid, *International Journal of Thermal and Sciences* 45 (2006) 706–715.
- [34] S.K. Mahapatra, B.K. Dandapat, A. Sarkar, Analysis of combined conduction and radiation heat transfer in presence of participating medium by the development of hybrid method, *Journal of Quantitative Spectroscopy and Radiative Transfer* 102 (2006) 277–292.
- [35] L.H. Liu, L.M. Ruan, H.P. Tan, On the treatment of open boundary condition for radiative transfer equation, *International Journal of Heat and Mass Transfer* 46 (2003) 181–183.
- [36] L.H. Liu, Domain isolation concept for solution of radiative transfer in large-scale semitransparent media, *Journal of Quantitative Spectroscopy and Radiative Transfer* 78 (2003) 373–379.